

SUPPORTING INFORMATION

for

The interplay between ceria particle size, reducibility, and activity for the selective oxidation of ethanol with ceria-supported gold catalysts

Gregory M. Mullen[†], Edward J. Evans Jr.[§], Benjamin C. Siegert[†], Nathaniel R. Miller[‡], Duan

Zhiyao[§], Benjamin K. Rosselet[†], Iliya Sabzevari[†], Adrianna Brush[†], Graeme Henkelman[§], and C.

Buddie Mullins^{†‡§}*

[†]McKetta Department of Chemical Engineering, The University of Texas at Austin, Austin,
Texas 78712, United States

[‡]Texas Materials Institute, The University of Texas at Austin, Austin, Texas 78712, United
States

[‡]Department of Geosciences, Jackson School of Geosciences, University of Texas at Austin,
Austin, TX 78712, United States

[§]Department of Chemistry, The University of Texas at Austin, Austin, Texas 78712, United
States

1. XRD spectra of ceria supports prior to gold deposition

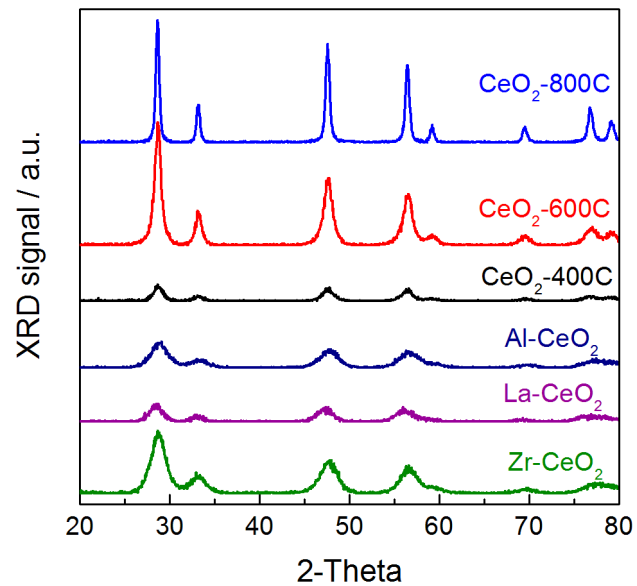


Figure S1. XRD spectra of ceria supports prior to gold deposition.

2. Representative STEM images of ceria supports prior to gold deposition and histograms of ceria particle size from STEM image analysis

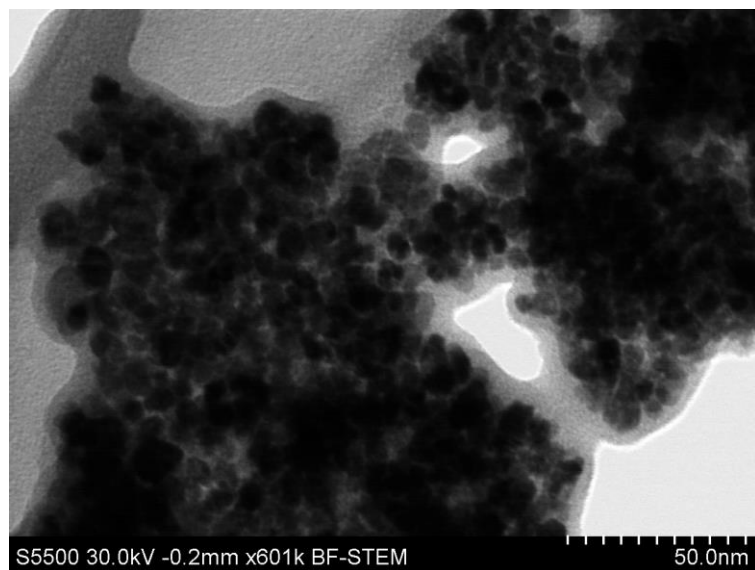


Figure S2. STEM image of CeO₂-400C

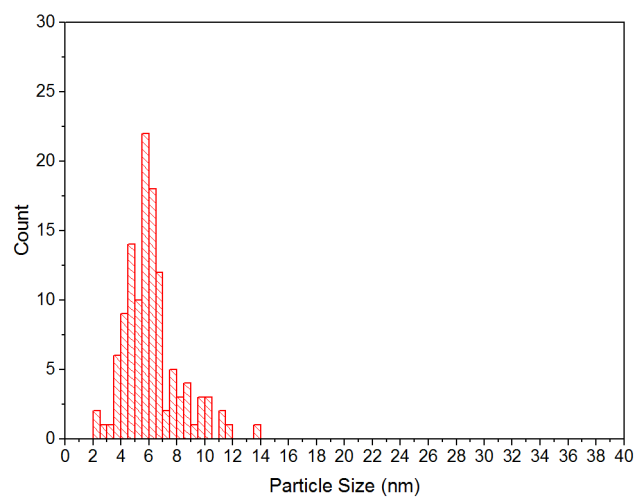


Figure S3. Histogram of particle size distribution for CeO₂-400C

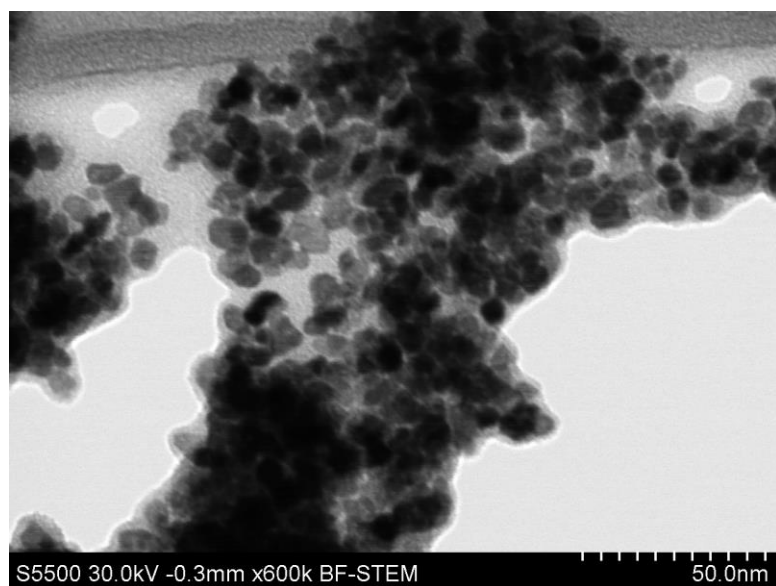


Figure S4. STEM image of CeO₂-600C

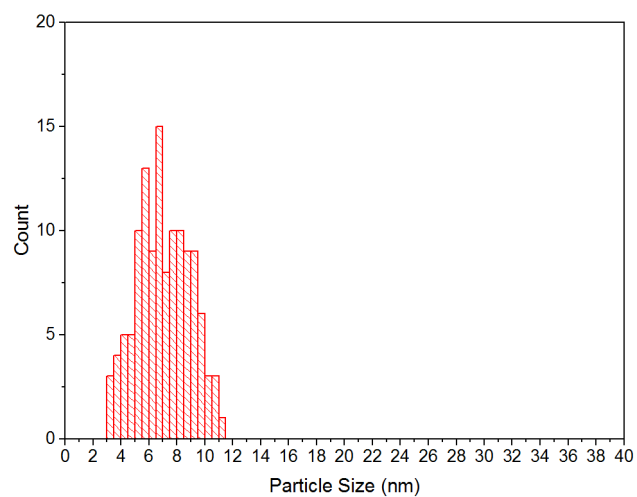


Figure S5. Histogram of particle size distribution for CeO₂-600C

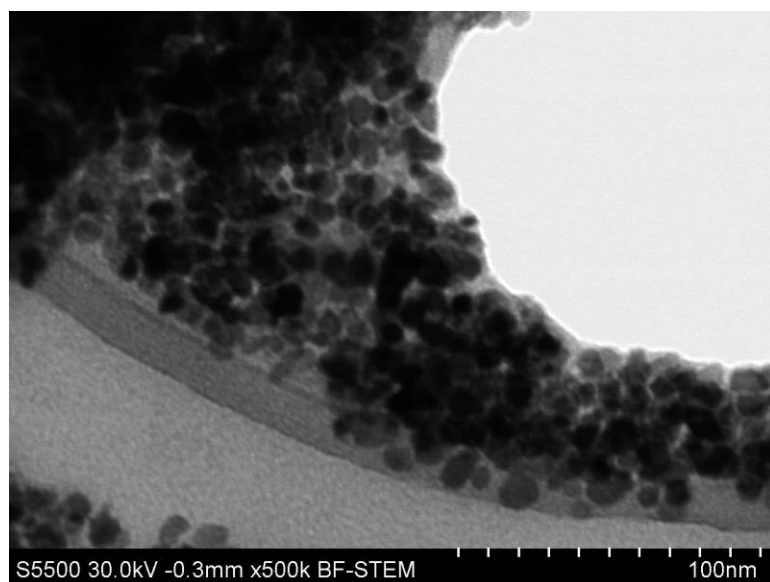


Figure S6. STEM image of CeO₂-800C

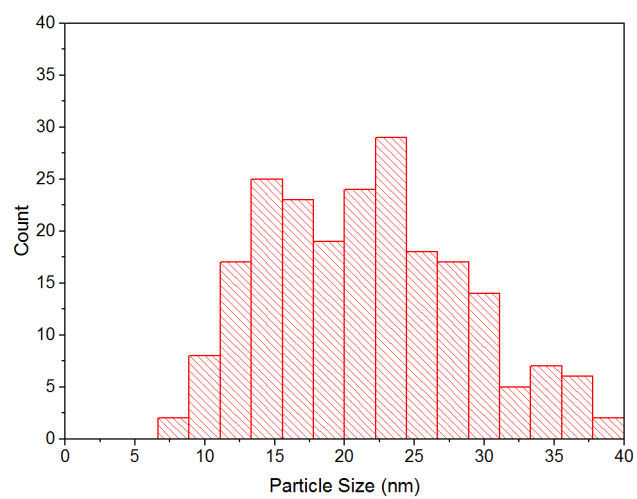


Figure S7. Histogram of particle size distribution for CeO₂-800C

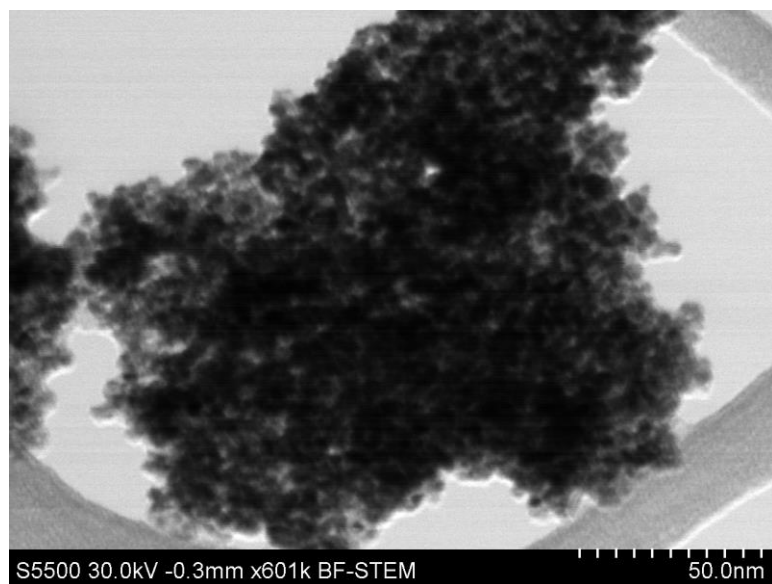


Figure S8. STEM image of Al-CeO₂

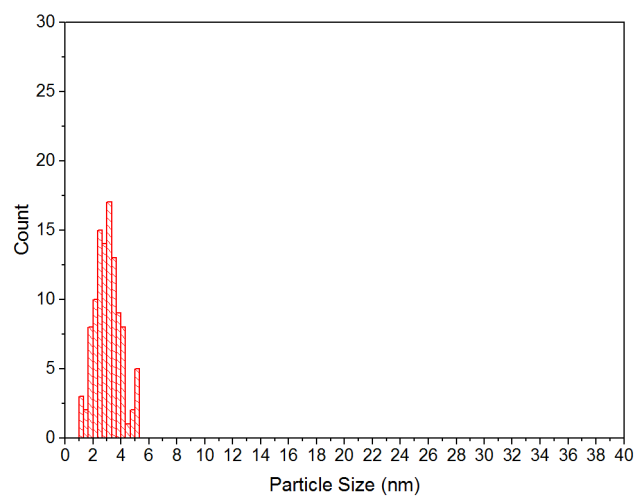


Figure S9. Histogram of particle size distribution for Al-CeO₂

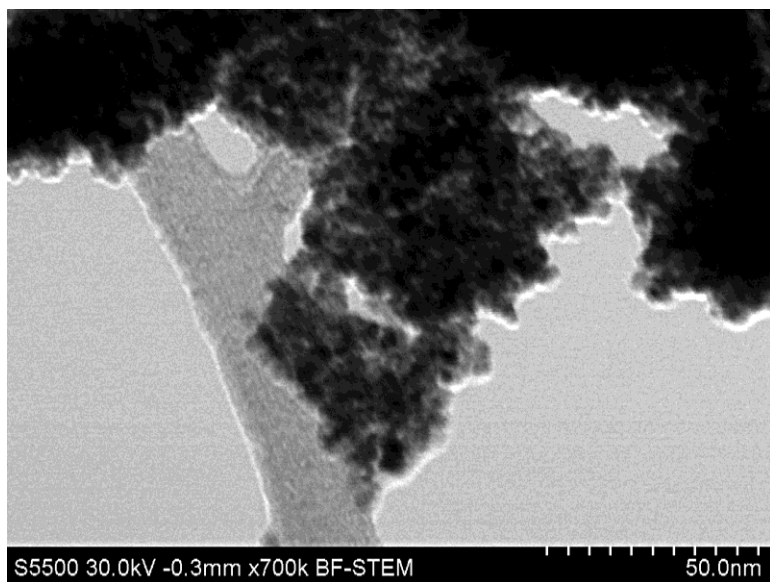


Figure S10. STEM image of La-CeO₂

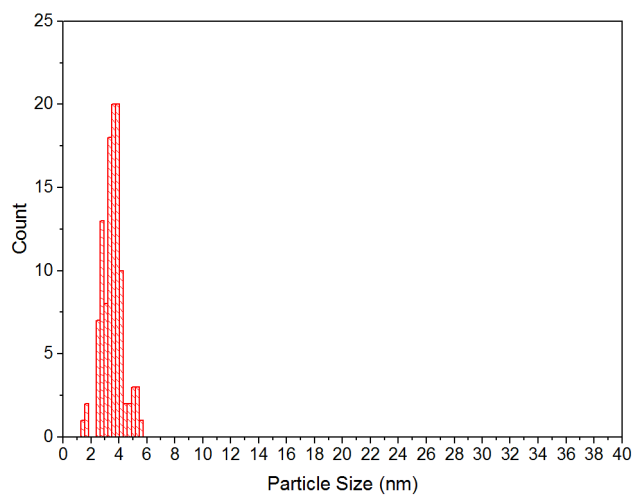


Figure S11. Histogram of particle size distribution for La-CeO₂

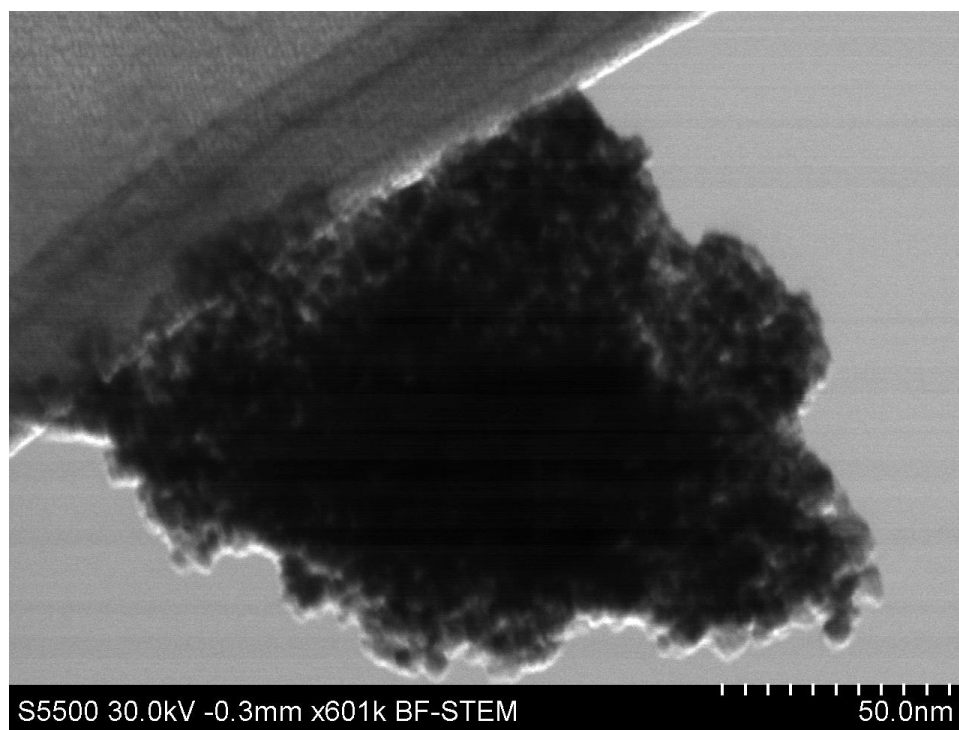


Figure S12. STEM image of Zr-CeO₂

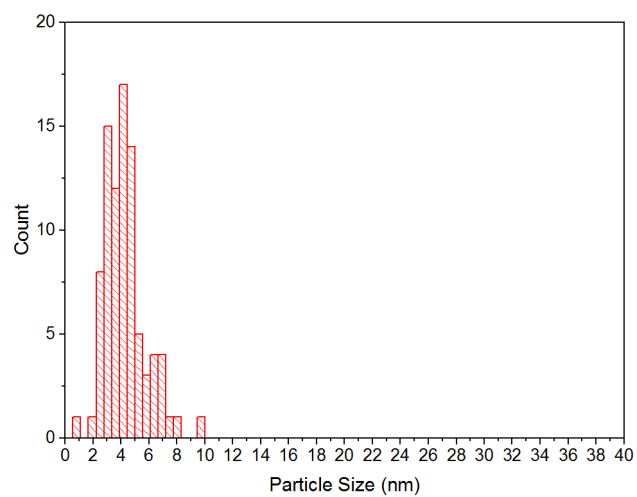


Figure S13. Histogram of particle size distribution for Zr-CeO₂

3. Analysis of Ce 3d XPS spectra for determination of Ce³⁺ species by method of Le Normand et al.

To quantitatively assess the amount of Ce³⁺ in the XPS spectrum for each Au/CeO₂ catalyst, we employed the method of Le Normand et al.,¹ which estimates the v''' peak area by measuring the u''' peak area and taking the ratio of v''' [$\frac{3}{2} I(u''') = I(v''')$] to the total area of the Ce 3d 5/2 peaks. The u''' peak does not overlap with other peaks in the 3d region and the v₀, v, v' and v'' peaks do not overlap with any of the 3d 3/2 peaks, therefore the area of the u''' the total area of the v₀, v, v' and v'' peaks can be measured unambiguously. By calculating v''' from the area of u''' and dividing this value by the total area of the 3d 5/2 features [$I(v''') + I(v_0, v, v', v'')$], a less ambiguous metric for analysis of changes to the concentration of Ce⁴⁺ in the material is obtained. This ratio equals 0.32 for pure CeO₂ and decreases as the amount of Ce³⁺ in the material increases.¹ The equation for this calculation is shown here:

$$\frac{I(v''')}{I(3d \frac{5}{2})} = \frac{\frac{3}{2} I(u''')}{\frac{3}{2} I(u''') + I(v_0, v, v', v'')}$$

Table S1. Ratios of v''' area to total area of features in the Ce 3d 5/2 XPS region

Sample	I(v''')/I(3d 5/2)
Au/CeO ₂ -400C	0.32
Au/CeO ₂ -600C	0.32
Au/CeO ₂ -800C	0.33
Au/Al-CeO ₂	0.34
Au/La-CeO ₂	0.31
Au/Zr-CeO ₂	0.32

4. BET surface area versus H₂ consumption from TPR for ceria support materials

To assess the correlation between surface area and H₂ consumption for the ceria support materials, for each material we plotted the specific surface area as determined by BET analysis against the specific H₂ consumption determined by integration of TPR patterns. We observed a strong correlation between surface area and H₂ consumption for the CeO₂-800C, CeO₂-600C, CeO₂-400C, and Zr-CeO₂ supports. The Al-CeO₂ and La-CeO₂ supports each exhibited lower H₂ consumption values per unit surface area.

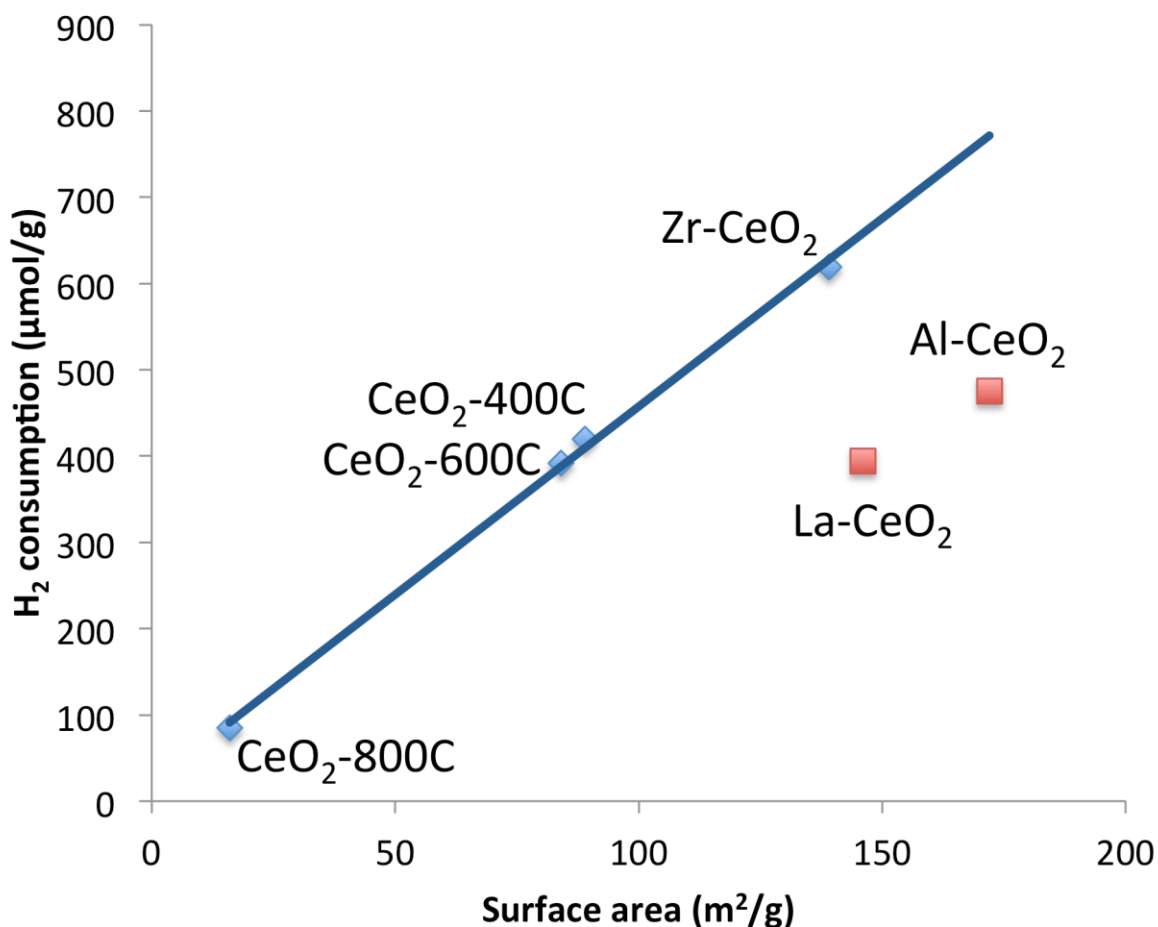


Figure S16. Plot of specific H₂ consumption versus specific surface area of the support materials

5. Calculation of the percent reduction of surface capping oxygen during H₂-TPR of Au/CeO₂ catalysts.

We calculated the atomic density of oxygen at the surface of the CeO₂ particles assuming that the surface consisted entirely of the CeO₂(111) facet. Ceria nanoparticles generally consist of octahedral and truncated octahedral particles predominantly exposing the (111) facet, which has the highest stability.² Using the lattice parameter of CeO₂, we calculated the surface density of oxygen of the (111) surface to be 1.31x10⁻⁵ mol. atoms/m². By multiplying this density by the specific surface area of each catalyst, we obtained the amount of surface capping oxygen per gram of material. Integrating the reduction features in the TPR spectra provided the specific amount of H₂ consumed by the material. Assuming that each mol. of H₂ reduced one mol. of surface oxygen, we calculated the percent of capping oxygen that would have been reduced during the TPR process. The calculation was conducted as follows:

$$\% \text{ reduction surface O} = \frac{X_{H_2}}{\rho_{O,surf} * SA}$$

X_{H2} = H₂ consumption during TPR [mol]

ρ_{O,surf} = surface density of oxygen on CeO₂ crystallites [1.31x10⁻⁵ mol/m²]

SA = specific surface area of material [m²/g]

6. Ethanol conversion data

Table S2. Ethanol conversion data for each catalyst tested in study

Sample	% conv. ethanol	Stdev
Au/CeO ₂ -400C	6.57%	0.01%
Au/CeO ₂ -600C	3.61%	0.37%
Au/CeO ₂ -800C	0.44%	0.10%
Au/Al-CeO ₂	10.13%	0.16%
Au/La-CeO ₂	9.58%	0.14%
Au/Zr-CeO ₂	7.17%	0.00%

7. Mears' criterion and the Weisz-Prater criterion for each catalyst during ethanol oxidation

Mears Criterion for External Mass Transfer

To gauge the relative effects of external mass transfer, we calculated the Mears Criterion for each catalyst under the steady state reaction conditions. External mass transfer effects can be neglected if the following criterion is met:

$$\frac{-r_A' r_b R n}{k_c C_{Ab}} < 0.15$$

r_A' – rate of reaction

ρ_b – bulk density of catalyst bed

R – radius of catalyst pellet

n – reaction order in ethanol

k_c – mass transfer coefficient

C_{Ab} – bulk concentration of ethanol

The Reynolds number is low, therefore k_c can be estimated from Sherwood number

$$Sh = k_c * 2R / D_e = 2$$

D_e – effective diffusivity of ethanol in air

Mears Criterion for External Heat Transfer

To gauge the relative effects of external heat transfer, we calculated the Mears Criterion for each catalyst under the steady state reaction conditions. External heat transfer effects can be neglected if the following criterion is met:

$$\left| \frac{-\Delta H_r (-r_A') r_b R E}{h_i T_b^2 R_g} \right| < 0.15$$

ΔH_r – enthalpy change of reaction

r_A' – rate of reaction

ρ_b – bulk density of catalyst bed

R – radius of catalyst pellet

E – activation energy

h – heat transfer coefficient

T_b – reaction temperature

R_g – gas constant

Reynolds number was low for our system, therefore we the heat transfer coefficient (h) estimated using the Nusselt number

$$Nu = h \cdot 2R / k_t = 2$$

k_t – thermal conductivity of reactant mixture (assumed to be air at 353 K)

Weisz-Prater Criterion for Internal Diffusion

To gauge the relative effects of external heat transfer, we calculated the Weisz-Prater Criterion for each catalyst under the steady state reaction conditions. Internal diffusion effects can be neglected if the following criterion is met:

$$C_{WP} = \frac{-r'_{A(obs)} r_c R^2}{D_e C_{As}} < 1$$

$r_{A(obs)}$ – rate of reaction

ρ_c – solid density of catalyst bed

R – radius of catalyst pellet

D_e – effective diffusivity of ethanol in air

C_{As} – surface concentration of ethanol

Table S3. Mears and Weisz-Prater coefficients associated with acetaldehyde production for each catalyst

Catalyst	Mears (mass transfer)	Weisz-Prater	Mears (heat transfer)
Au/CeO ₂ -400C	6.96E-02	1.24E-01	1.51E-02
Au/CeO ₂ -600C	6.84E-03	2.10E-01	2.48E-02
Au/CeO ₂ -800C	8.80E-04	3.38E-02	3.52E-03
Au/Al-CeO ₂	1.42E-01	2.54E-01	3.08E-02
Au/La-CeO ₂	1.29E-01	2.15E-01	2.55E-02
Au/Zr-CeO ₂	1.25E-01	1.92E-01	2.15E-02

8. Correlation between ethanol oxidation activity and surface area and between ethanol oxidation activity and H₂ consumption

We performed linear regression analysis to assess the correlation between H₂ consumption and acetaldehyde production activity and specific surface area and acetaldehyde production activity for the catalysts. The correlation between H₂ consumption and activity is stronger, as shown in Figure S16. This correlation strength becomes even more pronounced when the outlying point associated with the Au/CeO₂-800C catalyst is discarded, as shown in Figure S17.

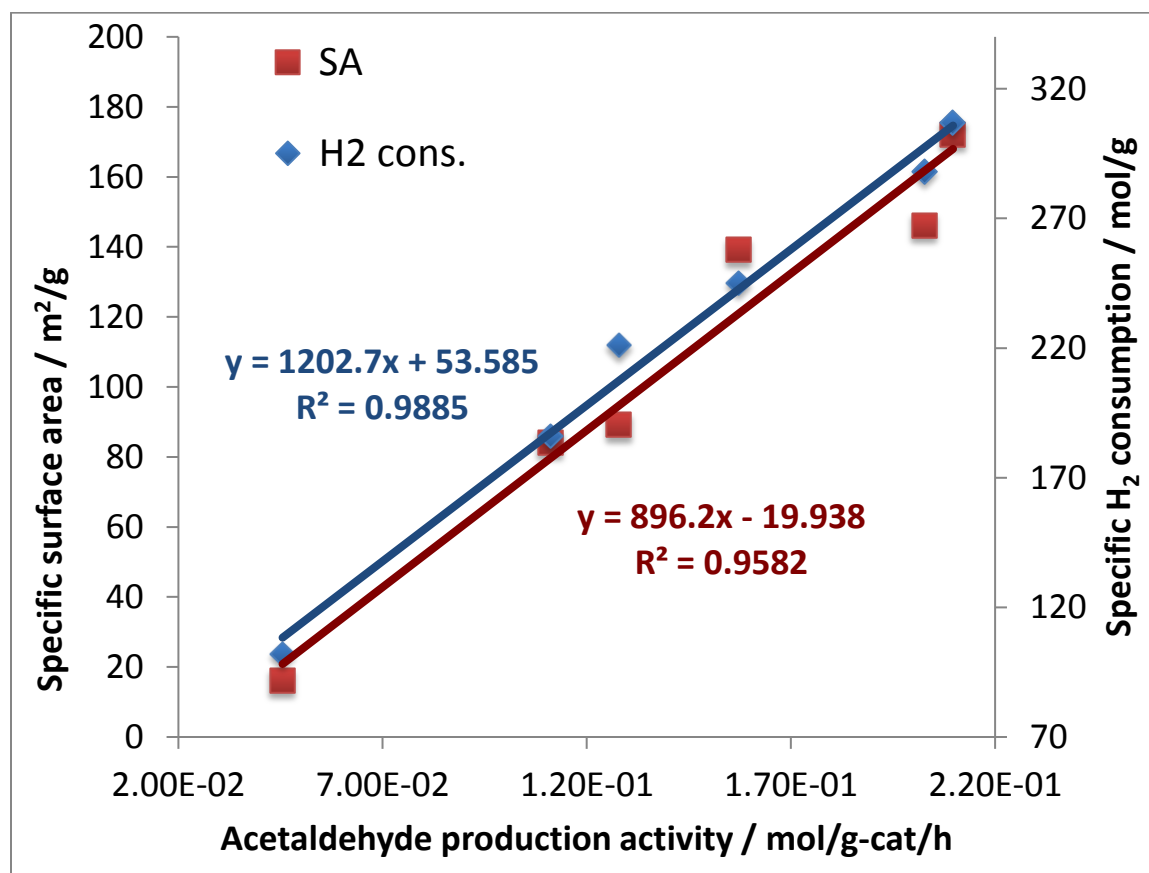


Figure S17. Results from linear regression of ethanol oxidation activity versus specific H₂ consumption of the catalysts and oxidation activity versus ethanol specific surface area.

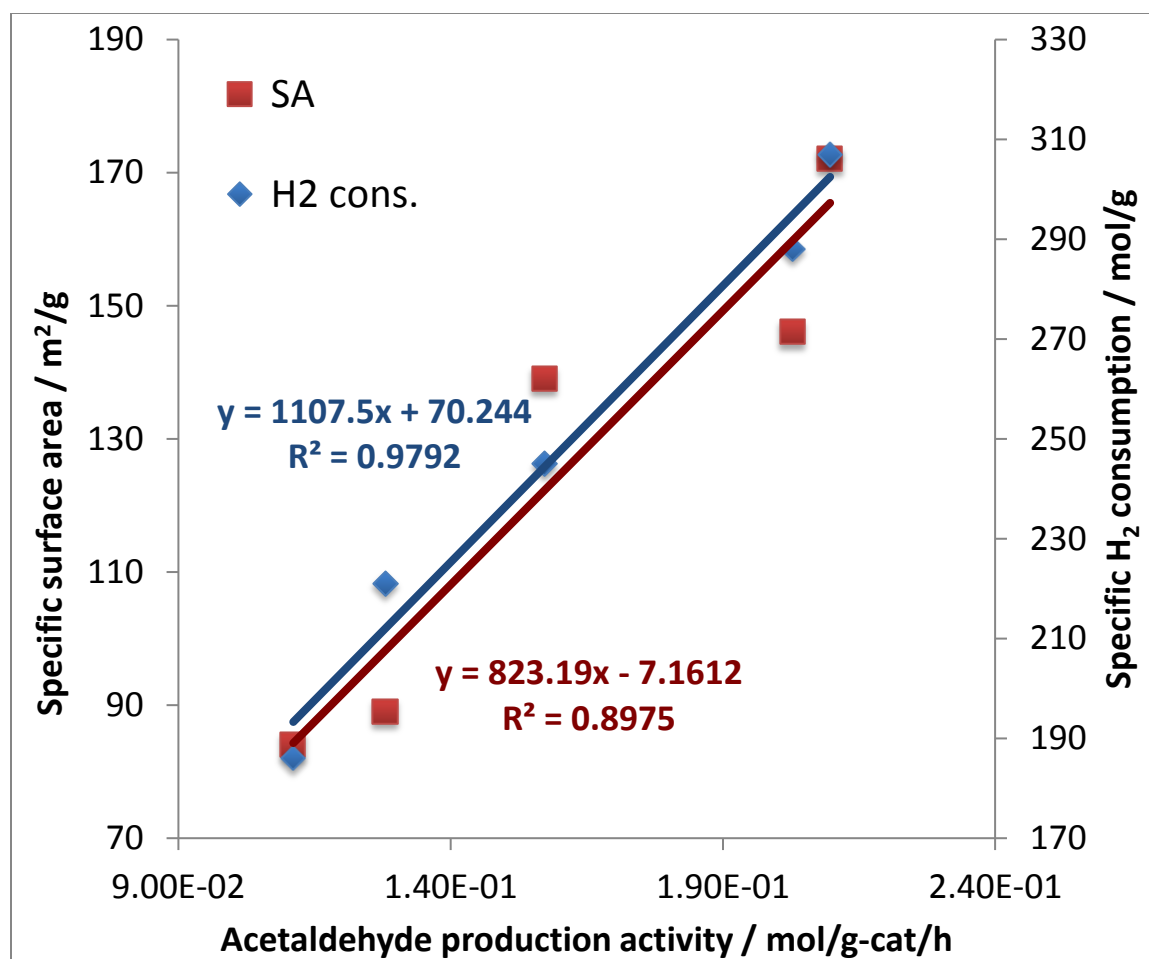


Figure S18. Results from linear regression of ethanol oxidation activity versus specific H₂ consumption of the catalysts and oxidation activity versus ethanol specific surface area after removal of outlying data points for Au/CeO₂-800C.

References

- 1 F. Le Normand, L. Hilaire, K. Kili, G. Krill and G. Maire, *J. Phys. Chem.*, 1988, **92**, 2561–2568.
- 2 D. Zhang, X. Du, L. Shi and R. Gao, *Dalt. Trans.*, 2012, **41**, 14455.